

# Synthetic Turbulence, Fractal Interpolation and Large-Eddy Simulation

Sukanta Basu,\* Efi Foufoula-Georgiou,<sup>†</sup> and Fernando Porté-Agel<sup>†</sup>  
*St. Anthony Falls Laboratory, University of Minnesota, Minneapolis, MN 55414*  
(Dated: May 22, 2019)

Fractal Interpolation has been proposed in the literature as an efficient way to construct closure models for the numerical solution of coarse-grained Navier-Stokes equations. It is based on synthetically generating a scale-invariant small-scale field and analytically evaluating its effects on large resolved scales. In this paper, we propose an extension of previous work by developing a multi-affine fractal interpolation scheme and demonstrate that it preserves not only the fractal dimension but also the higher-order structure functions and the non-Gaussian probability density functions of the velocity increments. The pertinence of this newly proposed method in the case of passive scalars is also shown.

PACS numbers: 47.27.Ak, 47.27.Eq, 47.53.+n

Keywords: Fractal, Intermittency, Large-Eddy Simulation, Passive Scalar, Turbulence

Generation of turbulence-like fields (also known as *Synthetic Turbulence*) has received considerable attention in recent years. Several schemes have been proposed [1, 2, 3, 4, 5] with different degrees of success in reproducing various characteristics of turbulence. Recently, Scotti and Meneveau [6, 7] further broadened the scope of synthetic turbulence research by demonstrating its potential in computational modeling. Their innovative turbulence emulation scheme based on the *Fractal Interpolation Technique* (FIT) [8, 9] was found to be particularly amenable for a specific type of turbulence modeling, known as Large-Eddy Simulation (LES, at present the most efficient technique available for high Reynolds number flow simulations, in which the larger scales of motion are resolved explicitly and the smaller ones are modeled). The underlying idea was to explicitly reconstruct the subgrid (unresolved) scales from given resolved scale values (assuming computation grid-size falls in the *inertial range* of turbulence) using FIT and subsequently estimate the relevant subgrid-scale (SGS) tensors necessary for LES. Simplicity, straightforward extensibility for multi-dimensional cases, and low computational complexity (appropriate use of *fractal calculus* can even eliminate the computationally expensive explicit reconstruction step, see [6, 7] for details) makes this FIT-based approach an attractive candidate for SGS modeling in LES.

Although the approach of [6, 7] is better suited for LES than any other similar schemes (e.g., [1, 2, 3, 4, 5]), it falls short in preserving the essential small-scale properties of turbulence, such as multi-affinity (will be defined shortly) and non-Gaussian characteristics of the probability density function (pdf) of velocity increments. It is the purpose of this work to improve the approach of [6, 7] in terms of realistic turbulence-like signal generation with all the aforementioned desirable characteristics. We will

further demonstrate the competence of our scheme in the emulation of passive-scalar fields.

The fractal interpolation technique is an iterative affine mapping procedure to construct a synthetic deterministic small-scale field (in general fractal provided certain conditions are met, see below) given a few large-scale interpolating points (anchor points). For an excellent treatise on this subject, the reader is referred to the book by Barnsley [9]. In this paper, we will limit our discussion (without loss of generality) only to the case of three interpolating data points:  $\{(x_i, u_i), i = 0, 1, 2\}$ . For this case, the fractal interpolation iterative function system (IFS) is of the form  $\{R^2; w_n, n = 1, 2\}$ , where,  $w_n$  have the following affine transformation structure:

$$w_n \begin{pmatrix} x \\ u \end{pmatrix} = \begin{bmatrix} a_n & 0 \\ c_n & d_n \end{bmatrix} \begin{pmatrix} x \\ u \end{pmatrix} + \begin{pmatrix} e_n \\ f_n \end{pmatrix}, \quad n = 1, 2. \quad (1)$$

To ensure continuity, the transformations are constrained by the given data points as follows:  $w_n \begin{pmatrix} x_0 \\ u_0 \end{pmatrix} = \begin{pmatrix} x_{n-1} \\ u_{n-1} \end{pmatrix}$  and  $w_n \begin{pmatrix} x_2 \\ u_2 \end{pmatrix} = \begin{pmatrix} x_n \\ u_n \end{pmatrix}$ , for  $n = 1, 2$ . The parameters  $a_n, c_n, e_n$  and  $f_n$  can be easily determined in terms of  $d_n$  (known as the vertical stretching factors) and the given anchor points  $(x_i, u_i)$  by solving a linear system of equations. The attractor of the above IFS,  $G$ , is the graph of a continuous function  $u : [x_0, x_2] \rightarrow R$ , which interpolates the data points  $(x_i, u_i)$ , provided the vertical stretching factors  $d_n$  obey  $0 \leq |d_n| < 1$ . In other words,

$$G = \{(x, u(x)) : x \in [x_0, x_2]\}, \quad \text{where,} \\ u(x_i) = u_i, \quad i = 0, 1, 2. \quad (2)$$

Moreover, if  $|d_1| + |d_2| > 1$  and  $(x_i, u_i)$  are not collinear, then the fractal (box-counting) dimension of  $G$  is the unique real solution  $D$  of  $|d_1| a_1^{D-1} + |d_2| a_2^{D-1} = 1$  (for rigorous proof see [8]). In the special case of three equally spaced points covering the unit interval  $[0, 1]$ , i.e.,  $x_0 = 0$ ,  $x_1 = 0.5$  and  $x_2 = 1$ , the parameters of the affine transformation kernel become:  $a_n = 0.5$ ;  $c_n =$

\*Electronic address: basus@msi.umn.edu

<sup>†</sup>Also at the National Centre for Earth Surface Dynamics.

$(u_n - u_{n-1}) - d_n (u_2 - u_0)$ ;  $e_n = x_{n-1}$ ;  $f_n = u_{n-1} - d_n u_0$ ;  $n = 1, 2$ . In this case, the solution for the fractal dimension ( $D$ ) becomes:

$$D = 1 + \log_2 (|d_1| + |d_2|) \quad (3)$$

Notice that the scalings  $d_1$  and  $d_2$  are free parameters and cannot be determined using only equation (3); at least one more constraint is necessary. For example, [6, 7] chose to use the additional condition:  $|d_1| = |d_2|$ .

Not long ago, it was found that turbulent velocity signals at high Reynolds numbers have a fractal dimension of  $D \simeq 1.7 \pm 0.05$ , very close to the value of  $D = \frac{5}{3}$  expected for Gaussian processes with a  $-\frac{5}{3}$  spectral slope [10]. For  $D = \frac{5}{3}$ , the assumption of  $|d_1| = |d_2|$  along with equation (3) yields  $|d_1| = |d_2| = 2^{-1/3}$  [6, 7]. One contribution of this paper is a robust way of estimating the stretching parameters without any ad-hoc prescription; the resulting synthetic field will not only preserve the fractal dimension ( $D$ ) but also other fundamental properties of real turbulence.

As an exploratory example, using the fractal interpolation IFS (equation 1), we construct a  $2^{17}$  points long synthetic fractal series,  $u(x)$ , with given coarse-grained points  $(0.0, 1.2)$ ,  $(0.5, -0.3)$  and  $(1.0, 0.7)$  and the stretching parameters used in [6, 7]:  $d_1 = -2^{-1/3}$ ,  $d_2 = 2^{-1/3}$ . Clearly, Figure 1a depicts that the synthetic series has fluctuations at all scales and it passes through all three interpolating points. Next, from this synthetic series we compute higher-order structure functions (see Figure 1b for orders 2, 4 and 6), where the  $q^{\text{th}}$ -order structure function,  $S_q(r)$ , is defined as follows:

$$S_q(r) = \langle |u(x+r) - u(x)|^q \rangle \sim r^{\zeta_q} \quad (4)$$

where, the angular bracket denotes spatial averaging and  $r$  is a distance that varies in an appropriate scaling region (known as the inertial range in turbulence). If the scaling exponent  $\zeta_q$  is a nonlinear function of  $q$ , then following the convention of [1, 2, 3, 4, 5], the field is called *multiaffine*, otherwise it is termed as *monoaffine*. In this context, we would like to mention that, Kolmogorov's celebrated 1941 hypothesis (a.k.a K41) based on the assumption of global scale invariance in the inertial range predicts that the structure functions of order  $q$  scale with an exponent  $\frac{q}{3}$  over inertial range separations [11, 12]. Deviations from  $\zeta_q = \frac{q}{3}$  would suggest inertial range intermittency and invalidate the K41 hypothesis. Inertial range intermittency is still an unresolved issue, although experimental evidence for its existence is overwhelming [11, 13]. To interpret the curvilinear behavior of the  $\zeta_q$  function observed in experimental measurements (e.g., [13]), Parisi and Frisch [12, 14] proposed the *multifractal* model, by replacing the global scale invariance with the assumption of local scale invariance. They conjectured that at very high Reynolds number, turbulent flows have singularities (almost) everywhere and showed that the

singularity spectrum is related to the structure function-based scaling exponents,  $\zeta_q$  by the Legendre transformation.

Our numerical experiment with the default stretching parameters of [6, 7], i.e.,  $|d_1| = |d_2| = 2^{-1/3}$ , revealed that the scaling exponents follow the K41 predictions (after ensemble averaging over one hundred realizations corresponding to different initial interpolating points), i.e.,  $\zeta_q = \frac{q}{3}$  (not shown here), a signature of monoaffine fields. Later on, we will give analytical proof that indeed this is the case for  $|d_1| = |d_2| = 2^{-1/3}$ . Also, in this case, the pdfs of the velocity increments,  $\delta u_r(x) = u(x+r) - u(x)$ , always portray near-Gaussian (slightly flatter core and lower flatness factors) behavior irrespective of  $r$  (see Figure 1c). This is contrary to the observations [11, 13], where, typically the pdfs of increments are found to be  $r$  dependent and become more and more non-Gaussian as  $r$  decreases. Theoretically, non-Gaussian characteristics of pdfs correspond to the presence of intermittency in the velocity increments and gradients (hence in the energy dissipation) [2, 5, 11, 12].

At this point, we would like to invoke an interesting mathematical result regarding the scaling exponent spectrum,  $\zeta_q$ , of the fractal interpolation IFS [15]:

$$\zeta_q = 1 - \log_N \sum_{n=1}^N |d_n|^q \quad (5)$$

where,  $N$  = the number of anchor points - 1 (in our case  $N = 2$ ). The original formulation of [15] was in terms of a more general scaling exponent spectrum,  $\tau(q)$ , rather than the structure function based spectrum  $\zeta_q$ . The  $\tau(q)$  spectrum is an exact Legendre transform of the singularity spectrum in the sense that it is valid for any order of moments (including negative) and any singularities [16, 17].  $\tau(q)$  can be reliably estimated from data by the Wavelet-Transform Modulus-Maxima method [16, 17]. To derive equation (5) from the original formulation, we made use of the equality:  $\tau(q) = \zeta_q - 1$ , which holds for positive  $q$  and for positive singularities of Hölder exponents less than unity [16, 17]. In turbulence, the most probable Hölder exponent is 0.33 (corresponding to the K41 value) and for all practical purposes the values of Hölder exponents lie between 0 and 1 (see [18, 19]). Hence the use of the above equality is well justified.

Equation (5) could be used to validate our previous claim, that the default parameters of [6, 7] give rise to a monoaffine field (i.e.,  $\zeta_q$  is a linear function of  $q$ ). If we consider  $|d_1| = |d_2| = d = 2^{-1/3}$ , then,  $\zeta_q = 1 - \log_2 (|d_1|^q + |d_2|^q) = 1 - \log_2 (2d^q) = -q \log_2 (d) = -q \log_2 (2^{-1/3}) = \frac{q}{3}$  [QED]. Equation (5) could also be used to derive the classic result of Barnsley regarding the fractal dimension of IFS. It is well-known [20, 21] that the graph dimension (or box-counting dimension) is related to  $\zeta_1$  as follows:  $D = 2 - \zeta_1$ . Now, using equation (5) we get,  $D = 2 - \zeta_1 = 1 + \log_N \sum_{i=1}^N |d_i|$ . For  $N = 2$ , we recover equation (3).

Intuitively, by prescribing several scaling exponents,  $\zeta_q$  (which are known apriori from observational data), it is possible to solve for  $d_n$  from the overdetermined system of equations (5). These solved parameters,  $d_n$ , along with other easily derivable (from the given anchor points and  $d_n$ ) parameters ( $a_n, c_n, e_n$  and  $f_n$ ) in turn can be used to construct multi-affine signals. For example, solving for the values quoted by Frisch [12]:  $\zeta_2 = 0.70, \zeta_3 = 1, \zeta_4 = 1.28, \zeta_5 = 1.53, \zeta_6 = 1.77, \zeta_7 = 2.01$  and  $\zeta_8 = 2.23$ , along with  $\zeta_1 = 0.33$  (corresponding to  $D = \frac{5}{3}$ ), yields the stretching factors  $|d_n| = 0.8868, 0.6763$ . There are altogether eight possible sign combinations for the above stretching parameter magnitudes and all of them can potentially produce multi-affine fields with the aforementioned scaling exponents. However, extensive numerical experimentation revealed that only the combinations:  $(-0.8868, 0.6763), (0.6763, -0.8868), (-0.8868, -0.6763)$  and  $(-0.6763, -0.8868)$  reproduce realistic turbulence signals (in terms of mimicking the pdfs of increments and the visual appearance of the series themselves). Although all the above four stretching combinations are quite suitable for synthetic turbulence generation, all of them might not be the “right” candidate from LES-performance perspective. Rigorous apriori and aposteriori testing of these stretching factors-based fractal SGS models is needed to elucidate this issue and this will be the subject of future research (details on LES SGS model testing can be found in the review article [22]).

We repeated our previous numerical experiment with the stretching parameters  $d_1 = -0.8868$  and  $d_2 = 0.6763$ . Figure 2a shows the measured values (ensemble averaged over one hundred realizations) of the scaling exponents  $\zeta_q$  up to 12<sup>th</sup> order. For comparison we have also shown the theoretical values computed directly from equation (5). A model proposed by She and Lévéque [23] based on a hierarchy of fluctuation structures associated with the vortex filaments is also shown for comparison. We chose this particular model because of its remarkable agreement with experimental data. The She and Lévéque model predicts:  $\zeta_q = \frac{q}{9} + 2 - 2 \left(\frac{2}{3}\right)^{\frac{q}{3}}$ . Figure 2b shows the pdfs of the increments, which is quite similar to what is observed in real turbulence – for large  $r$  the pdf is near Gaussian while for smaller  $r$  it becomes more and more peaked at the core with high tails (see also Figure 3 for the variation of flatness factors of increment pdfs with distance  $r$ ).

Our scheme could be easily extended for synthetic passive-scalar (any diffusive component in a fluid flow that has no dynamical effect on the fluid motion itself, e.g., a pollutant in air, temperature in a weakly heated flow, a dye mixed in a turbulent jet or moisture mixing in air [24, 25]) field generation. The statistical and dynamical characteristics (anisotropy, intermittency, pdfs etc.) of passive-scalars are surprisingly different from the underlying turbulent velocity field [24, 25]. For example, it is even possible for the passive-scalar field to exhibit intermittency in a purely Gaussian velocity

field [24, 25]. Similar to the K41, neglecting intermittency, the Kolmogorov-Obukhov-Corrsin (KOC) hypothesis predicts that at high Reynolds and Peclet numbers, the  $q^{th}$ -order passive-scalar structure function will behave as:  $\langle |\theta(x+r) - \theta(x)|^q \rangle \sim r^{\frac{q}{3}}$  in the inertial range. Experimental observations reveal that analogous to turbulent velocity, passive-scalars also exhibit anomalous scaling (departure from the KOC scaling). Observational data also suggest that passive-scalar fields are much more intermittent than velocity fields and result in stronger anomaly [24, 25].

To generate synthetic passive-scalar fields, we need to determine the stretching parameters  $d_1$  and  $d_2$  from prescribed scaling exponents,  $\zeta_q$ . Unlike the velocity scaling exponents, the published values (based on experimental observations) of higher-order passive-scalar scaling exponents display significant scatter. Thus for our purpose, we used the predictions of a newly proposed passive-scalar model [26]:  $\zeta_q = 2 + \left(\frac{8}{9}\right)^2 - 2 \left(\frac{3}{4}\right)^{q/6} - \left(\frac{8}{9}\right)^2 \left(\frac{7}{16}\right)^{q/2}$ . This model based on the hierarchical structure theory of [23] shows reasonable agreement with the observed data. Moreover, unlike other models, this model manages to predict that the scaling exponent  $\zeta_q$  is a nondecreasing function of  $q$ . Theoretically, this is very crucial, because, otherwise, if  $\zeta_q \rightarrow -\infty$  as  $q \rightarrow +\infty$ , the passive-scalar field cannot be bounded [12, 26].

Employing equation (5) and the scaling exponents (upto 8<sup>th</sup>-order) predicted by the above model, we get the following stretching factors:  $|d_n| = 0.9644, 0.6060$ . As before, we found that only the combinations  $(-0.9644, 0.6060), (0.6060, -0.9644), (-0.9644, -0.6060)$  and  $(-0.6060, -0.9644)$  generate satisfactory fields. We again repeated the previous numerical experiment, now with the stretching parameter combination:  $d_1 = -0.9644$  and  $d_2 = 0.6060$ . Like before, we compared the estimated [using equation (4)] scaling exponents from one hundred realizations with the theoretical values [from equation (5)] and the agreement was found to be highly satisfactory. To check whether a generated passive-scalar field ( $d_1 = -0.9644, d_2 = 0.6060$ ) possesses more non-Gaussian characteristics than its velocity counterpart ( $d_1 = -0.8868, d_2 = 0.6763$ ), we performed a simple numerical experiment. We generated both the velocity and passive-scalar fields from identical anchor points and computed the corresponding flatness factors,  $K$ , as a function of distance  $r$  (see Figure 3). Evidently, the passive-scalar field exhibits stronger non-Gaussian behavior than the velocity field, in accord with the literature.

In this paper, we proposed a simple yet efficient scheme to generate synthetic turbulent velocity and passive-scalar fields. This method is competitive with most of the other synthetic turbulence emulator schemes (e.g., [1, 2, 3, 4, 5]). As far as limitations, like other methods (except [3]) our proposed scheme cannot reproduce the small-scale skewness behavior of velocity fields. It has been observed that in the inertial range the skewness is approximately  $-0.3$  to  $-0.4$  (K41 predicts a value

of  $-0.28$ ) and this small negative value is believed to be the origin of vortex stretching and nonlinear energy transfer from large to small scales (a.k.a the energy cascade) [3, 5]. On the positive side, the proposed method could be easily implemented as a SGS model in LES following [6, 7]. Potentially, SGS models based on fractal interpolation can address some of the unresolved issues in LES: they can systematically account for the effects of near-wall proximity and atmospheric stability on the SGS dynamics. Of course, this would require some kind of universal dependence of the scaling exponents on both wall-normal distance and stability. Quest for these kinds of universality has began only recently [27, 28].

## Acknowledgments

We thank Alberto Scotti, Charles Meneveau, Venugopal Vuruputur and Boyko Dodov for useful discussions. The first author is indebted to Jacques Lévy-Véhel for his generous help. This work was partially funded by NSF and NASA grants. One of us (SB) was partially supported by the Doctoral Dissertation Fellowship from the University of Minnesota. All the computational resources were kindly provided by the Minnesota Supercomputing Institute. All these supports are greatly appreciated.

---

[1] T. Vicsek and A. L. Barabási, *J. Phys. A.* **24**, L845 (1991).

[2] R. Benzi, L. Biferale, A. Crisanti, G. Paladin, M. Vergassola, and A. Vulpiani, *Physica D* **65**, 352 (1993).

[3] A. Juneja, D. P. Lathrop, K. R. Sreenivasan, and G. Stolovitzky, *Phys. Rev. E* **49**, 5179 (1994).

[4] L. Biferale, G. Boffetta, A. Celani, A. Crisanti, and A. Vulpiani, *Phys. Rev. E* **57**, R6261 (1998).

[5] T. Bohr, M. H. Jensen, G. Paladin, and A. Vulpiani, *Dynamical Systems Approach to Turbulence*, (Cambridge University Press, Cambridge, UK, 1998).

[6] A. Scotti and C. Meneveau, *Phys. Rev. Lett.* **78**, 867 (1997).

[7] A. Scotti and C. Meneveau, *Physica D* **127**, 198 (1999).

[8] M. F. Barnsley, *Constr. Approx.* **2**, 303 (1986).

[9] M. F. Barnsley, *Fractals Everywhere*, (Academic Press, Boston, MA, 1993).

[10] A. Scotti, C. Meneveau, and S. G. Saddoughi, *Phys. Rev. E* **51**, 5594 (1995).

[11] K. R. Sreenivasan and R. A. Antonia, *Ann. Rev. Fluid Mech.* **29**, 435 (1997).

[12] U. Frisch, *Turbulence: The Legacy of A. N. Kolmogorov*, (Cambridge University Press, Cambridge, UK, 1995).

[13] F. Anselmet, Y. Gagne, E. J. Hopfinger, and R. A. Antonia, *J. Fluid Mech.* **140**, 63 (1984).

[14] G. Parisi and U. Frisch, in *Proceedings of the International School on Turbulence and Predictability in Geophysical Fluid Dynamics and Climate Dynamics*, M. Ghil, R. Benzi, and G. Parisi (North-Holland, Amsterdam, 1985).

[15] J. Lévy-Véhel, K. Daoudi, and E. Lutton, *Fractals* **2**, 1 (1994).

[16] J. F. Muzy, E. Bacry, and A. Arneodo, *Phys. Rev. E* **47**, 875 (1993).

[17] S. Jaffard, *SIAM J. Math. Anal.* **28**, 944 (1997).

[18] E. Bacry, A. Arneodo, U. Frisch, Y. Gagne, and E. Hopfinger, in *Turbulence and Coherent Structures*, edited by O. Métais and M. Lesieur (Kluwer, 1990).

[19] M. Vergassola, R. Benzi, L. Biferale, and D. Pisarenko, *J. Phys. A.* **26**, 6093 (1993).

[20] B. Mandelbrot, *Fractals: Form, Chance, and Dimension*, (W. H. Freeman, New York, NY, 1977).

[21] A. Davis, A. Marshak, W. Wiscombe, and R. Cahalan, *J. Geophys. Res.* **99**, 8055 (1994).

[22] C. Meneveau and J. Katz *Ann. Rev. Fluid Mech.* **32**, 1 (2000).

[23] Z. S. She and E. L. Lévéque *Phys. Rev. Lett.* **72**, 336 (1994).

[24] Z. Warhaft, *Ann. Rev. Fluid Mech.* **32**, 203 (2000).

[25] B. I. Shraiman and E. D. Siggia, *Nature* **405**, 639 (2000).

[26] Q. Z. Feng, *Phys. Fluids* **14**, 2019 (2002).

[27] G. Ruiz-Chavarria, S. Ciliberto, C. Baudet, and E. Lévéque, *Physica D* **141**, 183 (2000).

[28] K. G. Aivalis, K. R. Sreenivasan, Y. Tsuji, J. C. Klewicki, C. A. Biltoft, *Phys. Fluids* **14**, 2439 (2002).

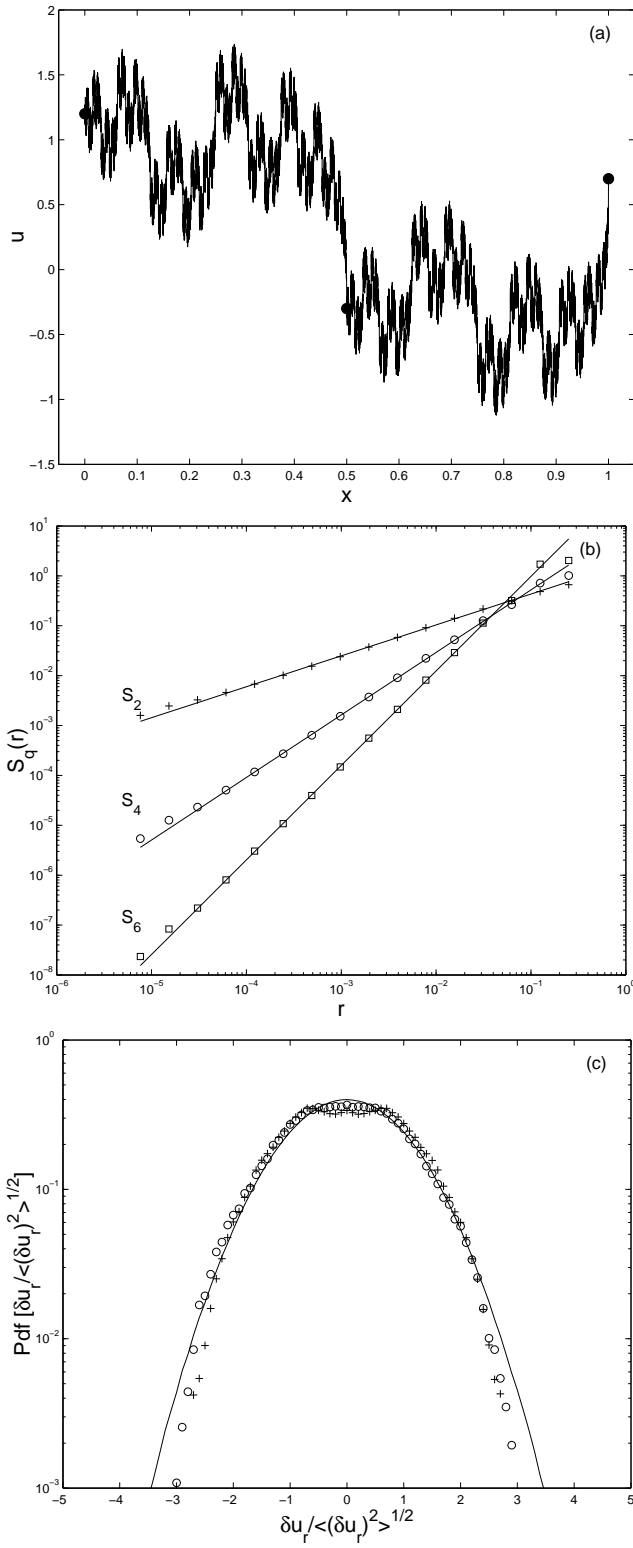


FIG. 1: (a) A synthetic turbulence series of fractal dimension  $D = \frac{5}{3}$ . The black dots denote initial interpolating points. (b) Structure functions of order 2, 4 and 6 (as labeled) computed from the series in Figure 1a. The slopes ( $\zeta_q$ ) corresponding to this particular realization are 0.62, 1.25 and 1.89, respectively. (c) Pdfs of the normalized increments of the series in Figure 1a. The plus signs correspond to  $r = 2^{-14}$ , while the circles refer to a distance  $r = 2^{-6}$ . The solid curve designates the Gaussian distribution for reference.

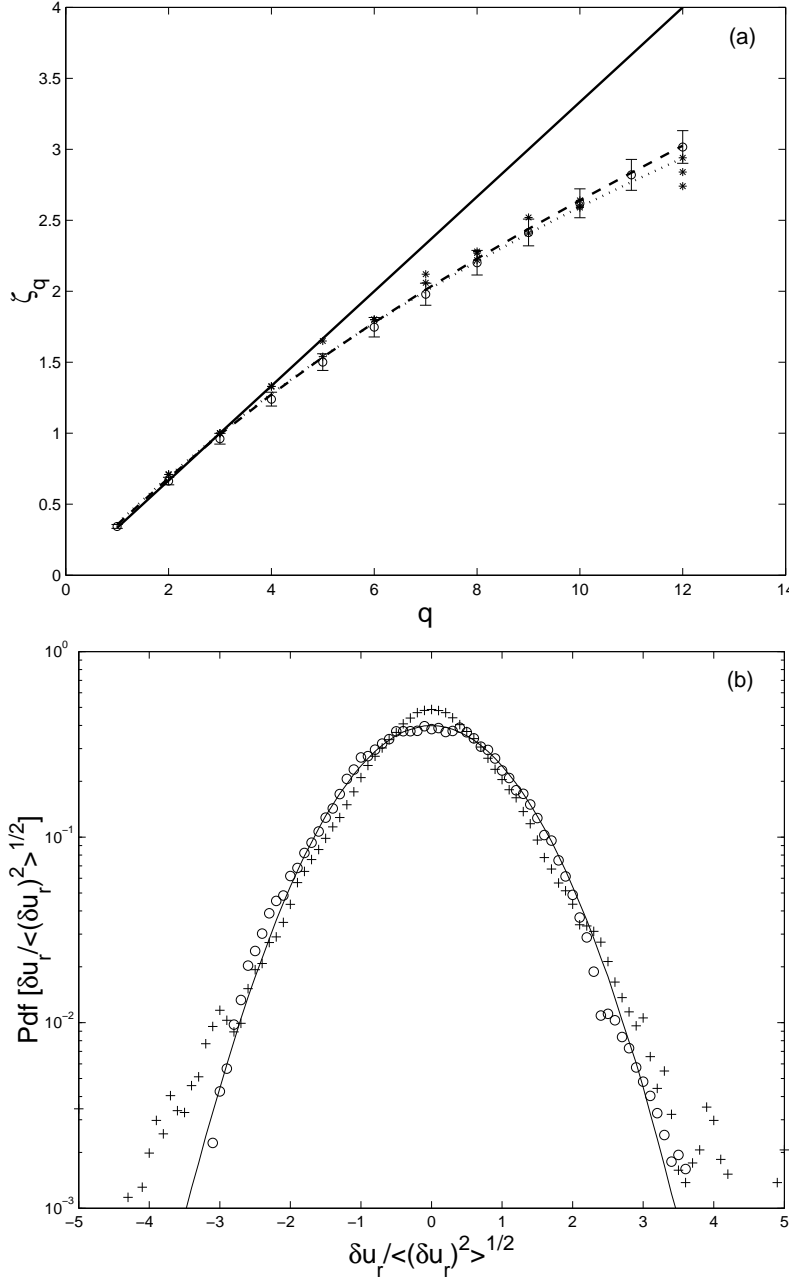


FIG. 2: (a) The scaling exponent function  $\zeta_q$ . The continuous, dashed and dotted lines denote the K41, equation (5), and the She-Léveque model predictions respectively. The circles with error bars (one standard deviation) are estimated values over one hundred realizations using  $d_1 = -0.8868$  and  $d_2 = 0.6763$ . Experimental data of Anselmet et al.'s [5] is also shown for reference (star signs). (b) Pdfs of the normalized increments of the multiaffine series. The plus signs denote  $r = 2^{-14}$ , while the circles refer to a distance  $r = 2^{-6}$ . The solid curve designates the Gaussian distribution for reference.

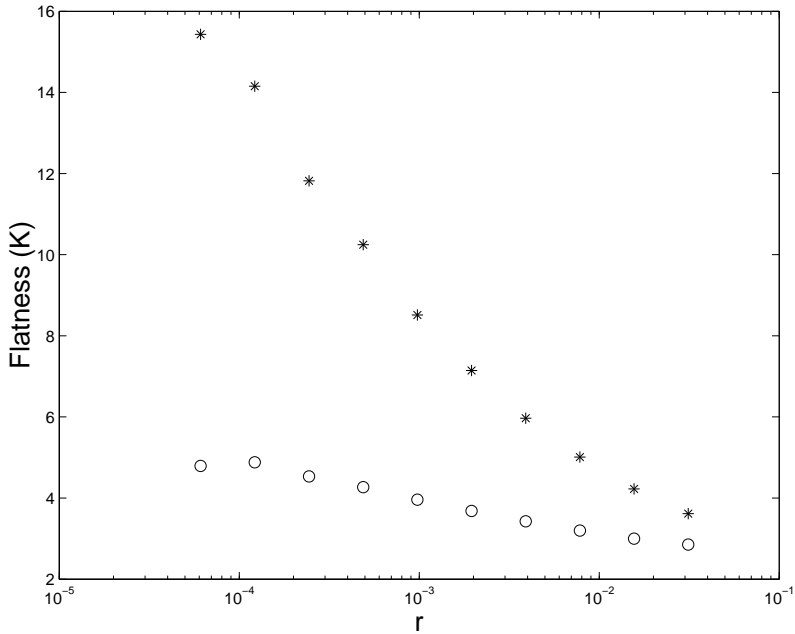


FIG. 3: The flatness factors of the pdfs of the increments of the velocity (circles) and passive-scalar field (stars) as a function of distance  $r$ . Note that both the fields approach the Gaussian value of 3 only at large separation distances. Clearly the passive-scalar field is more non-Gaussian than the velocity field.